

Free-space discrete-variable quantum key distribution in a mountainous environment

Xing-Ran Chen(陈星燃), Jian-Hong Shi(史建红), and Hai-Long Zhang(张海龙)

Citation: Chin. Phys. B, 2025, 34 (**5**): 050301. DOI: 10.1088/1674-1056/adbd25
Journal homepage: http://cpb.iphy.ac.cn; http://iopscience.iop.org/cpb

What follows is a list of articles you may be interested in

Deep-learning-assisted optical communication with discretized state space of structured light

Minyang Zhang(张敏洋), Dong-Xu Chen(陈东旭), Pengxiang Ruan(阮鹏祥), Jun Liu(刘俊), Dong-Zhi Fu(付栋之), Jun-Long Zhao(赵军龙), and Chui-Ping Yang(杨垂平)
Chin. Phys. B, 2024, 33 (**12**): 120304. DOI: 10.1088/1674-1056/ad8553

Performance analysis of quantum key distribution using polarized coherent-states in free-space channel

Zengte Zheng(郑增特), Ziyang Chen(陈子扬), Luyu Huang(黄露雨),Xiangyu Wang(王翔宇), and Song Yu(喻松)
Chin. Phys. B, 2023, 32 (**3**): 030306. DOI: 10.1088/1674-1056/ac7450

Analysis of atmospheric effects on the continuous variable quantum key distribution

Tao Liu(刘涛), Shuo Zhao(赵硕), Ivan B. Djordjevic, Shuyu Liu(刘舒宇), Sijia Wang(王思佳), Tong Wu(吴彤), Bin Li(李斌), Pingping Wang(王平平), and Rongxiang Zhang(张荣香)
Chin. Phys. B, 2022, 31 (**11**): 110303. DOI: 10.1088/1674-1056/ac6b1f

Short-wave infrared continuous-variable quantum key distribution over satellite-to-submarine channels

Qingquan Peng(彭清泉), Qin Liao(廖骎), Hai Zhong(钟海), Junkai Hu(胡峻凯), and Ying Guo(郭迎)
Chin. Phys. B, 2022, 31 (**6**): 060306. DOI: 10.1088/1674-1056/ac490a

Experimental simulation of violation of the Wright inequality by coherent light

Feng Zhu(朱锋), Wei Zhang(张巍), Yidong Huang(黄翊东)
Chin. Phys. B, 2017, 26 (**10**): 100302. DOI: 10.1088/1674-1056/26/10/100302

SPECIAL TOPIC — Quantum communication and quantum network

Free-space discrete-variable quantum key distribution in a mountainous environment

Xing-Ran Chen(陈星燃), Jian-Hong Shi(史建红), and Hai-Long Zhang(张海龙)†

Henan Key Laboratory of Quantum Information and Cryptography, SSF, IEU, Zhengzhou 450001, *China*

(Received 29 November 2024; revised manuscript received 5 March 2025; accepted manuscript online 6 March 2025)

Free-space quantum key distribution (QKD) offers broader geographical coverage and more flexible system deployment than fiber-based systems. However, the free-space environment is highly complex, and various attenuation factors can significantly reduce the key distribution efficiency or even lead to encoding failures. This paper discusses and analyzes the impact of turbulence and fog in mountainous environments on free-space discrete-variable quantum key distribution. Through numerical simulation, this study examines the effects of altitude and visibility on transmittance and turbulence intensity, finding that turbulence intensity decreases with increasing altitude while transmittance increases; improvements in visibility also lead to increased transmittance. Beam wandering due to turbulence is also dominant. Combining these factors, the effects on the total transmittance and the secret key rate are taken into consideration. Our work could provide a reference for the deployment of practical QKD systems in actual mountainous environments.

Keywords: free-space, DV-QKD, mountainous environment, secret key rate

PACS: 03.67.Dd, 03.67.Hk, 03.67.–a

DOI: 10.1088/1674-1056/adbd25 **CSTR:** 32038.14.CPB.adbd25

1. Introduction

Distinct from classical cryptography, which depends on computational complexity[1] for security, quantum key distribution (QKD)[2,3] leverages fundamental quantum mechanical principles such as the non-cloning theorem to achieve unconditional security, allowing authorized parties to securely share secret keys. Based on whether the encoding spatial dimension of the quantum states is finite, QKD protocols can be categorized into discrete-variable quantum key distribution (DV-QKD)[4] and continuous-variable quantum key distribution (CV-QKD).[5] DV-QKD encodes on discrete variables, such as the polarization and phase of photons. The first DV-QKD protocol, BB84, utilizes the polarization of single photons for encoding.[6] In CV-QKD, the information carriers are no longer the polarization or phase of single photons but rather the canonical components of the light field, such as position and momentum in phase space.[7]

QKD systems require the support of communication channels,[8] which can generally be divided into optical fiber channels and free-space channels. Compared with optical fiber channels, free-space channels can achieve broader geographical coverage and more flexible system deployment. However, free-space channels are less resistant to interference and more susceptible to the impact of the external environment, thus the quantum states are easily affected. Turbulence,[17] rain, fog[13] and snow in free space can all affect the transmission channel, making it necessary to establish models that integrate with the actual environment. Some typical environments, such as mountainous environments, maritime atmospheric environments and urban environments, have different impacts on free-space QKD, and the factors that need to be considered are varied.

Mountainous environments[10] are typical natural environments, generally referring to highlands above an altitude of 500 m, with significant undulations, steep slopes and a reticulated distribution. The main characteristics, such as pronounced altitude variations, large temperature differences during day and night and extensive vegetation, are all key factors affecting free-space DV-QKD.

In this paper, based on the scenario of free-space QKD in a mountainous environment and its characteristics, we considered factors such as altitude, turbulence, fog and beam wandering.[12] We have studied the impact of these factors on average transmittance and key rate both separately and in combination. The paper is organized as follows. In Section 2, we describe the effects of turbulence and fog on channel transmittance. In Sections 3 and 4, we derive the secret key rate of two decoy states in the BB84 protocol, combining the mentioned factors and concluding the integrated influences on the key rate. The conclusion is drawn in Section 5.

†Corresponding author. E-mail: zhhl049@126.com

© 2025 Chinese Physical Society and IOP Publishing Ltd. All rights, including for text and data mining, AI training, and similar technologies, are reserved.

2. Turbulence and fog effects on free-space channels

2.1. Effect of turbulence on average transmittance

Turbulence in free-space channels primarily arises from random fluctuations in the atmospheric refractive index. These fluctuations induce several effects on the transmitted beam, including intensity attenuation, beam wandering, beam broadening and scintillation,[17] all of which degrade the beam quality at the receiver and may even disrupt the encoding process. Due to randomness, direct measurement of the magnitude of turbulence is complicated. However, the degree of refractive index fluctuation can reflect the intensity of the turbulence, and the refractive index is related to temperature. We can infer the strength of turbulence from the magnitude of the refractive index.

By calculating near-field and far-field mean irradiation intensity, we can estimate the mean transmittance. The average transmittance is given by[9,11]

$$T_{\mathrm{t}} = \frac{T_0}{T_1}, \tag{1}$$

where T_0 is the initial pulse half-width, T_1 is the pulse half-width at the receiver and can be described as

$$T_1 = \sqrt{T_0^2 + 8a_1}. \tag{2}$$

Here, $a_1 = 0.39 C_{\mathrm{n}}^2 L L_0^{5/3} c^{-2}$ [9] with C_{n}^2 is the refractive index structure constant, L is the propagation distance in km and c is the speed of light in vacuum.

In a mountainous environment, we consider that the intensity of turbulence is mainly affected by the altitude and wind speed. An equation in terms of altitude and wind speed can be derived utilizing the Hufnagel–Valley model[14,17]

$$\begin{aligned} C_{\mathrm{n}}^2(h) \;=\; & A\exp(-h/100) + 5.94\times 10^{-53}(v/27)^2 h^{10} \\ & \times \exp(-h/1000) + 2.7\times 10^{-16}\exp(-h/1500), \end{aligned} \tag{3}$$

where A is the nominal value of C_{n}^2 at the ground, v is the estimated high-altitude wind speed in m/s and h is the mean altitude in m. A commonly used value for A is 1.7×10^{-14}. Simultaneously, the wind speed is different when altitude is varied and can be written as[18]

$$v = v_0 \left(\frac{h}{h_0}\right)^n, \tag{4}$$

where v_0 is the wind speed at altitude h_0, which is the reference height. In this work we take $h_0 = 100$ m as the initial condition and n is used to describe the roughness of the ground surface; it has values of 0.23 (a number of trees, few buildings), 0.28 (forest with several villages) and 0.4 (tall buildings), respectively. We take 0.28 in this work.

Due to the significant temperature difference between nighttime and daytime in mountainous areas, it is usually considered that the turbulent strength is weak during the night compared with daytime. Consequently, the impact on the transmitted beam also differs from daytime conditions. Here, we have taken into account the HV-night model,[15] which has been adjusted and modified based on the Hufnagel–Valley model with parameter optimizations, it can be expressed as

$$\begin{aligned} C_{\mathrm{n}}^2(h) \;=\; & 1.9\times 10^{-15}\exp(-h/100) + 8.16\times 10^{-54} h^{10} \\ & \times \exp(-h/1000) + 3.02\times 10^{-17}\exp(-h/1500). \end{aligned} \tag{5}$$

The turbulent strength is independent of wind speed because the temperature fluctuation is relatively slight, which can lead to wind speed variation during the night. Based on Eqs. (3)–(5), the relationship between C_{n}^2 and altitude is shown in Fig. 1.

Figure 1 shows the variation of turbulence intensity with altitude during different times of the day. The results indicate that the refractive index structure constant decreases with increasing altitude during both day and night, suggesting that turbulence intensity decreases as altitude increases. The turbulence intensity during the day is significantly stronger than at night, and it gradually levels off with increasing altitude, transitioning from moderate to weak turbulence. When the altitude is around 5000 m, there is a slight elevation of the turbulence intensity.

Substituting C_{n}^2 into Eqs. (1) and (2), we can depict the variation of transmittance with the altitude and transmission distance.

From Figs. 2(a) and 2(b), the results show that link transmittance increases as the altitude increases under different transmission distances, and increasing distance results in transmittance reduction at the same altitude. Collectively, we have better mean transmittance at nighttime compared with daytime because the turbulent strength is not as strong during the day as during the night.

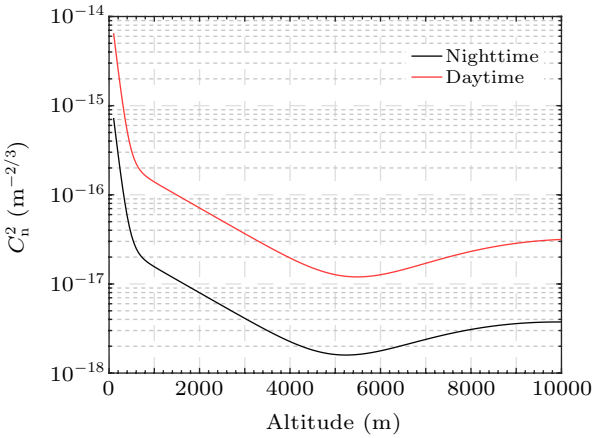


Fig. 1. Refractive index structure constant C_{n}^2 versus altitude ($n = 0.28$).

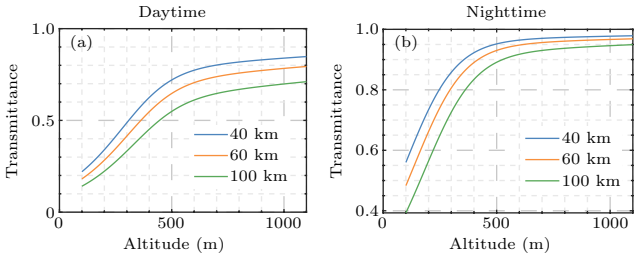


Fig. 2. Transmittance variation for different altitudes and times. (a) and (b) Corresponding daytime and nighttime during one day, where $T_0 = 10^{-14}$, $L_0 = 0.4$ and propagation distance $L = 40$ km, 60 km and 100 km, respectively.

2.2. Effects of fog on the average transmittance

Fog consists of numerous water droplets[16] that scatter, refract, diffract and extinguish light as a laser beam interacts with them. Consequently, foggy conditions attenuate optical signals in free-space communication, reducing QKD efficiency and potentially causing communication interruptions. The scattering effect is mainly considered; this influences channel transmittance when fog exists.

Generally, we can categorize scattering primarily into two types: Rayleigh scattering and Mie scattering.[13] Rayleigh scattering occurs when the laser wavelength is bigger than the particle size, and Mie scattering occurs if the wavelength is comparable to particle size. The radius of fog droplets is between 0.5 μm and 2 μm which makes Mie scattering the main scattering mechanism. We can express average transmittance as[13]

$$T_{\mathrm{f}} = \mathrm{e}^{-\beta L}, \tag{6}$$

where L is the propagation distance in km. β is the attenuation coefficient associated with visibility and wavelength, and is given by the Kruse model[19]

$$\beta = \frac{3.91}{V}\left(\frac{\lambda}{550}\right)^{-d}, \tag{7}$$

where V is the visibility in km, λ is the wavelength in nm and d is the size distribution coefficient of scattering. For different visibility ranges, the parameter d can be expressed as[21]

$$d = \begin{cases} 1.6, & V > 50 \text{ km}, \\ 1.3, & 6 \text{ km} < V < 50 \text{ km}, \\ 0.585V^{\frac{1}{3}}, & V < 6 \text{ km}. \end{cases} \tag{8}$$

According to Eqs. (6)–(8), the relationship between average transmittance and visibility can be derived for different ranges of visibility.

Figure 3 shows higher transmittance with better visibility. Moreover, the transmittance exhibits an exponential trend under low visibility, while it approximates a linear variation under moderate visibility. In particular, we can see that near a visibility of 6 km, the transmittance experiences a discontinuous increase because the variable d is no longer a function of visibility but a constant.

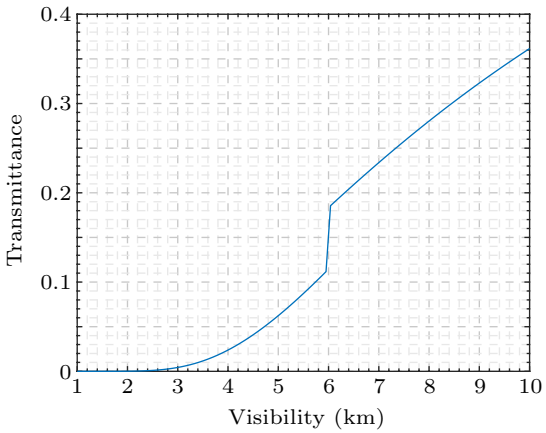


Fig. 3. Transmittance variation with visibility in the presence of fog with different visibility ranges (low visibility thick fog, $V \leq 6$ km and moderate visibility light fog, 6 km $< V \leq 10$ km), where $L = 10$ km and $\lambda = 1550$ nm.

3. The comprehensive effect of channel transmittance

Another significant effect of atmospheric turbulence is beam wandering. When turbulence is sufficiently strong, the transmitted beam breaks into multiple patches at the receiving plane, making it difficult to accurately describe the drift of the beam center relative to the center of the receiving plane. In the case of moderate and weak turbulence, beam wandering losses are dominant. Some models such as elliptic-beam and log-normal models are widely used. Here, we introduce the circle-beam model that is based on the elliptic-beam model[22] and is shown in Fig. 4.

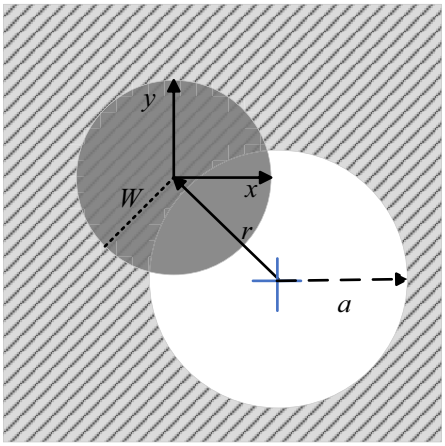


Fig. 4. Circle-beam model, where a is the radius of the receiver plane, W is the radius of the receiving beam at the plane and r is the wandering distance.

As represented in Fig. 4, the beam spot fluctuates around the aperture center after propagation through the free-space channel and the transmission efficiency is affected by fluctuation. We can derive transmission efficiency at the receiver plane according to the approximate expression of the incomplete Weber integral[20] as[22]

$$T^2 = T_{\mathrm{m}}^2 \mathrm{e}^{-(r/R)^{\lambda}}, \tag{9}$$

where $T_{\rm m}$ is the maximal transmission coefficient for the given beam-spot radius W at the receiver plane with the following form:[22]

$$T_{\rm m}^2 = 1 - {\rm e}^{-2a^2/W^2}, \tag{10}$$

where a is the aperture radius of the receiver plane. The shape and scale parameters, λ and R, can be expressed as follows:[22]

$$\lambda = 8\frac{a^2}{W^2}\frac{\exp(\frac{-4a^2}{W^2})I_1(\frac{4a^2}{W^2})}{1-\exp(\frac{-4a^2}{W^2})I_0(\frac{4a^2}{W^2})} \times \left[\ln\left(\frac{2T_{\rm m}^2}{1-\exp(\frac{-4a^2}{W^2})I_0(\frac{4a^2}{W^2})}\right)\right]^{-1}, \tag{11}$$

$$R = a\left[\ln\left(\frac{2T_{\rm m}^2}{1-\exp(\frac{-4a^2}{W^2})I_0(\frac{4a^2}{W^2})}\right)\right]^{-1/\lambda}, \tag{12}$$

where I_i is the modified Bessel function of the ith order. Due to the random fluctuations caused by beam wandering on the receiving plane, the fluctuating range conforms to the Weibull distribution and the probability distribution of the transmission coefficient is given by[22]

$$P(T) = \frac{2R^2}{\sigma^2\lambda T}\left(2\ln\frac{T_{\rm m}}{T}\right)^{\frac{2}{\lambda}-1} \times \exp\left[-\frac{1}{2\sigma^2}R^2\left(2\ln\frac{T_{\rm m}}{T}\right)\frac{2}{\lambda}\right], \tag{13}$$

where σ is the beam-wandering variance. We can express the transmission efficiency on the receiving plane through the average transmittance in Eq. (1). Combining Eqs. (10)–(13), the total transmittance of the channel in a mountainous environment is given by

$$T_{\rm mountain} = T_{\rm t}P(T_{\rm t})T_{\rm f}. \tag{14}$$

For the total transmittance of the channel, we primarily consider two periods of time during a day, before dawn and after sunrise. Environmental temperatures gradually decrease in the early morning, leading to easier condensation of water vapor in the air into liquid droplets and the formation of fog, which reduces visibility to a lower level; after sunrise, the increase in temperature causes the evaporation of water vapor, leading to a gradual increase in visibility and a noticeable decrease in fog density compared with the early morning hours. Figure 5 shows the variation of total transmittance with altitude and visibility.

In Fig. 5(a), the transmittance rises rapidly with increase in visibility. When the altitude is below 300 m, the transmittance experiences a slight increase as the altitude increases. Due to the absence of sunlight and lower environmental temperatures in the early morning, which do not change rapidly, the refractive index of the air remains at a relatively stable level, leading to weaker turbulence. Therefore, at this time, the main factor affecting transmittance is fog, with turbulence having a very minimal impact. However, in Fig. 5(b), when the altitude is below 500 m, the transmittance increases with increase in altitude and visibility, at which point fog and turbulence act jointly. When the altitude exceeds 500 m, the increase in altitude causes transmittance to level off and the trend of transmittance increasing with visibility is faster than below 500 m, indicating that the primary influencing factor is fog at this moment.

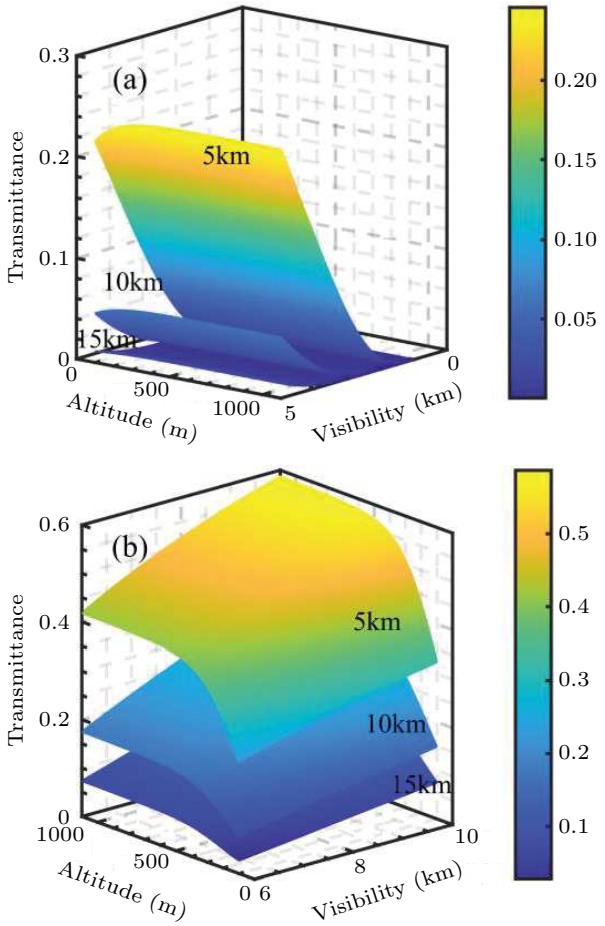


Fig. 5. (a) Variation of total transmittance with altitude and visibility before dawn. (b) Variation of total transmittance with altitude and visibility after sunrise. $L = 5$ km, 10 km and 15 km, respectively, $a = 50$ cm and $W = 0.2a$.

4. Secret key rate of free-space DV-QKD

In this section, we analyze the key rate of free-space DV-QKD in a practical system using the weak + vacuum two-decoy-states BB84 protocol,[24,25] Wang and Lo[24–27] proposed the decoy-state protocol and the multiple-decoy-state protocol in 2005, along with rigorous security proofs. These advances increased the secure key rate and the maximum secure distance of the QKD system. As a result, the use of decoy states in the BB84 protocol has become a common choice in actual QKD systems.

The secret key rate can be expressed as[23]

$$R = q\{-Q_\mu f(E_\mu)H_2(E_\mu) + Q_1^{L,\upsilon,0}[1 - H_2(e_1^{U,\upsilon,0})]\}, \quad (15)$$

where $H(x) = -x\log_2(x) - (1-x)\log_2(1-x)$ is the binary Shannon information function. q has different values for different protocols: here $q = 1/2$ in BB84. $f(x)$ is the bidirectional error correction efficiency, $Q_1^{L,\upsilon,0}$ is the lower bound of single photon gain and can be written as[24]

$$Q_1^{L,\upsilon,0} = \frac{\mu^2 \mathrm{e}^{-\mu}}{\mu\upsilon - \upsilon^2}\left(Q_\upsilon \mathrm{e}^{\upsilon} - Q_\mu \mathrm{e}^{\mu}\frac{\upsilon^2}{\mu^2} - \frac{\mu^2 - \upsilon^2}{\mu^2}Y_0\right), \quad (16)$$

where Y_0 is the dark count rate, Q_μ and Q_υ are the gains of the μ-signal state and υ-decoy state, respectively, and can be expressed as[25]

$$Q_\mu = \sum_{i=0}^{\infty} Y_i \frac{\mu^i}{i!}\mathrm{e}^{-\mu} = Y_0 + 1 - \mathrm{e}^{-\eta\mu}, \quad (17)$$

$$Q_\upsilon = \sum_{i=0}^{\infty} Y_i \frac{\upsilon^i}{i!}\mathrm{e}^{-\upsilon} = Y_0 + 1 - \mathrm{e}^{-\eta\upsilon}, \quad (18)$$

where η represents the total transmittance of the channel, which consists of several components: the transmittance at the receiver $\eta_\mathrm{B} = t_\mathrm{Bob}\eta_\mathrm{D}$, t_Bob is the transmittance of the internal optical path in the detector and η_D is the detector efficiency. Combining with Eq. (14), we can calculate the transmittance as $T_\mathrm{total} = T_\mathrm{mountain}\eta_\mathrm{B} = T_\mathrm{mountain}t_\mathrm{Bob}\eta_\mathrm{D}$. The error rate of μ, υ-photon state is given as follows:[25]

$$e_\mu = \frac{e_0 Y_0 + e_\mathrm{detector}(1 - \mathrm{e}^{-\eta\mu})}{Q_\mu}, \quad (19)$$

$$e_\upsilon = \frac{e_0 Y_0 + e_\mathrm{detector}(1 - \mathrm{e}^{-\eta\upsilon})}{Q_\upsilon}. \quad (20)$$

The $e_1^{U,\upsilon,0}$ is the upper-bound of the single photon bit error rate, which can be written as[24]

$$e_1^{U,\upsilon,0} = \frac{E_\upsilon Q_\upsilon e^{\upsilon} - e_0 Y_0}{Y_1^{L,\upsilon,0}\upsilon}, \quad (21)$$

where

$$\begin{aligned} Y_1^{L,\upsilon,0} &= Y_1^{L,\upsilon_1,\upsilon_2}|_{\upsilon_2\to 0} \\ &= \frac{\mu}{\mu\upsilon - \upsilon^2}\left(Q_\upsilon e^{\upsilon} - Q_\mu e^{\mu}\frac{\upsilon^2}{\mu^2} - \frac{\mu^2 - \upsilon^2}{\mu^2}Y_0\right). \end{aligned}$$

We will assume that the background is random. Thus the error rate of the background is $e_0 = 1/2$. e_detector is the probability that a photon hits an erroneous detector. Combining the overall transmittance and key rate formulae derived above, the comprehensive effects on the key rate at different altitudes and visibility levels during various time periods in mountainous areas are discussed.

First, the variation of the key rate across different altitude ranges after sunrise is illustrated in Fig. 6.

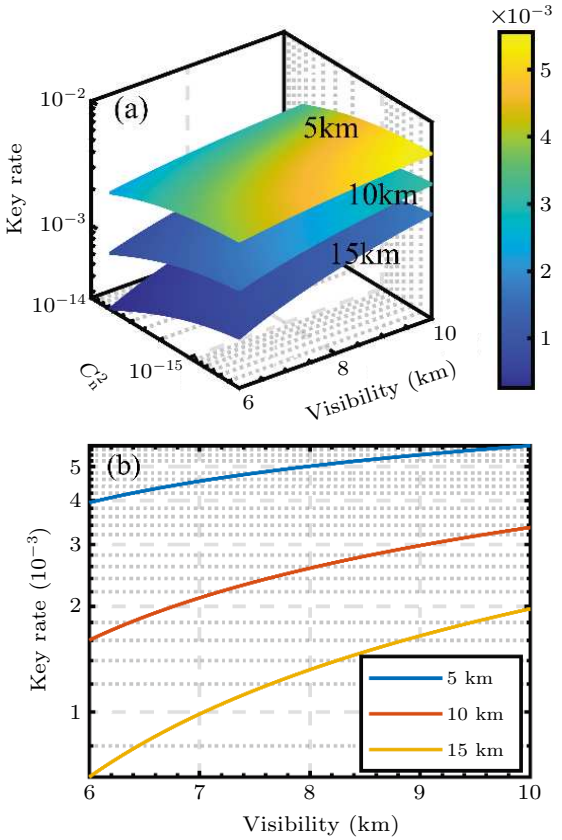


Fig. 6. (a) Variation of key rate with C_n^2, visibility and propagation distance when the altitude is below 500 m. (b) Key rate variation with visibility and transmission distance above 500 m. $\mu = 0.1$, $\upsilon = 0.05$, $Y_0 = 1.7 \times 10^{-5}$, $f = 2$, $\eta_\mathrm{B} = 0.4$, $\eta_\mathrm{D} = 0.15$ and $e_\mathrm{det} = 0.033$.

When the altitude is below 500 m, based on the conclusions drawn earlier, the transmittance is influenced by both turbulence and fog. Therefore, we also consider that the key rate is affected by the combined influence of turbulence and fog, as shown in Fig. 6(a). Under different transmission distances, both the decrease in turbulence intensity and the increase in visibility have a positive impact on the key rate, with the key rate reaching its maximum value under conditions of low turbulence and high visibility. As the transmission distance increases, the effect of turbulence becomes more pronounced. In Fig. 6(b), we mainly consider attenuation due to fog based on the visibility when the altitude exceeds 500 m. The key rate increases with the rise in visibility after sunrise under different transmission distances; at the same visibility level, the key rate decreases as the transmission distance increases.

Second, during the early morning hours, since the impact of turbulence on transmittance is not obvious when the altitude is below 300 m, and fog is the main influencing factor when the altitude is above 300 m, the key rate is considered to be primarily affected by fog during this time period.

Figure 7 shows that the secret key rate increases when visibility increases; when visibility drops to a certain level, the key rates for all three transmission distances experience a rapid decline. From the comprehensive analysis above, it is

important that in mountainous environments different factors need to be considered at different times and across different altitude ranges in practical QKD systems.

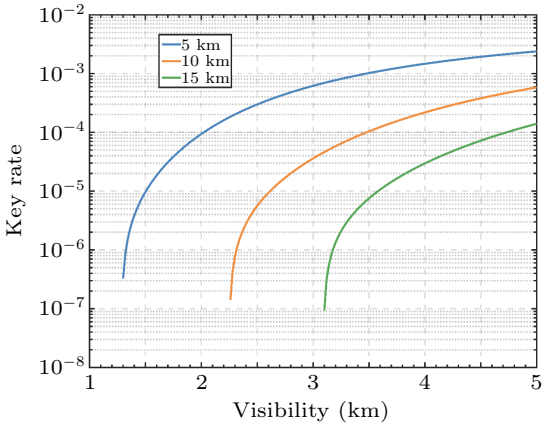


Fig. 7. Key rate variation with visibility at different propagation distances before dawn. $\mu = 0.1$, $\upsilon = 0.05$, $Y_0 = 1.7 \times 10^{-5}$, $f = 2$, $\eta_{\mathrm{B}} = 0.4$, $\eta_{\mathrm{D}} = 0.15$ and $e_{\mathrm{det}} = 0.033$.

5. Conclusion

In this paper, we have discussed the impact of mountainous environments on free-space DV-QKD. By considering the unique characteristics of mountainous regions, we have analyzed the effects of turbulence and fog on system performance. Firstly, the intensity of turbulence during the daytime is significantly greater than at night, and it gradually decreases with the increase in altitude; the impact of fog is mainly reflected in visibility, with better visibility leading to higher transmittance. Secondly, the turbulence effect causes the beam to drift on the receiving plane, which we represent using the Weibull distribution. We combined all the mentioned influencing factors and concluded that the comprehensive channel transmittance is less affected by turbulence at night, with fog being the main influencing factor; during the daytime, when the altitude is below 500 m, transmittance is jointly influenced by turbulence and fog. As altitude increases and visibility improves, transmittance also increases. When the altitude is above 500 m, transmittance is mainly affected by fog, and at this time the impact of visibility is more pronounced than when the altitude is below 500 m. In practical applications, different altitudes can be chosen based on visibility to improve channel transmittance. We also analyzed the impact of fog and turbulence on the secret key rate, and concluded that during the daytime at altitudes below 500 m affected by turbulence and fog the key rate decreases as the turbulence intensity diminishes and increases with a rise in visibility. The longer transmission distance makes the effects of turbulence and fog more obvious; when the altitude exceeds 500 m, the primary influencing factor is fog. During the nighttime, the effects of fog are dominant and the key rate drops sharply as visibility decreases. Our work could provide a reference for the deployment of QKD systems in actual natural environments. In future studies of free-space QKD it will be essential to select more comprehensive and primary parameters based on the characteristics of the actual environment when developing models, as this ensures that the models more accurately reflect real-world conditions.

References

[1] Bennett C H, Brassard G, Popescu S, *et al.* 1995 *Phys. Rev. Lett.* **76** 722
[2] Wang Y, Bao W S and Li H W 2014 *Chin. Phys. B* 23 080803
[3] Zhao Y B, Han Z F, Chen J J, Gu Y Z and Guo G C 2008 *Chin. Phys. Lett.* 25 3138
[4] Yin Z Q, Han Z F, Chen W, Xu F X, Wu Q L and Guo G C 2008 *Chin. Phys. Lett.* 25 3547
[5] Liu W Q, Peng J, Huang P, Wang S and Wang T 2018 *Chin. Phys. B* 27 070305
[6] Primaatmaja W I, Liang C C and Zhang G 2022 *Quantum Journal* **6** 613
[7] Guo H, Li Z Y and Peng X 2016 *Quantum Cryptography* (Beijing: National Defense Industry Press)
[8] Vasylyev D, Semenov A A, Vogel W, *et al.* 2017 *Phys. Rev. A* **96** 043856
[9] Young C Y, Andrews L C and Ishimaru A 1998 *Appl. Opt.* **37** 765560
[10] Liu Y, Yue W Z, Fan P L, Zhang Z T and Huang J N 2017 *Ecological Indicators* **81** 048
[11] Kelly D and Andrews L C 1999 *Waves Random Media* **9** 307
[12] Vaslylyev D, Semenov A A and Vogel W 2016 *Phys. Rev. Lett.* **117** 090501
[13] Sherif G, Heba A.F, Ahmed A and Moustafa H 2016 *Sixth International Conference on Digital Information Processing and Communications (ICDIPC), Beirut, Lebanon* pp. 151–155
[14] George C 1980 *Appl. Opt.* **19** 574
[15] Parenti R R and Sasiela R J 1994 *Opt. Soc. Am. A* **11** 288
[16] Muhammad S A, Laszlo C H, Sajid S M, *et al.* 2009*Journal of Communications* **4** 8
[17] Ricklin J, Hammel S, Eaton F, *et al.* 2006 *Opti. Fiber. Common. Rep* **3** 10297
[18] Tar K 2008 *Renewable and Sustainable Energy Reviews* **12** 014
[19] Mohammed N A, Wakeel A and Mostafa H A 2012 *International Journal of Video and Image Processing and Network* **12** 1
[20] Matest M A and Michail S M 1971 *Theory of Incomplete Cylindrical Functions and their Applications* (Berlin, Springer)
[21] Nadeem F, Flecker B, Leitgeb E, *et al.* 2008 *6th International Symposium on Communication Systems, Networks and Digital Signal Processing*, July 25–25, 2008, Graz, Austria, pp. 278–282
[22] Vasylyev D, Semenov A A and Vogel W 2012 *Phys. Rev. Lett.* **108** 220501
[23] Gottesman D, Lo H K, Lutkenhaus N and Preskill J 2004 *Quantum Inf. Comput.* **4** 325
[24] Ma X F, Qi B, Zhao Y and Lo H K 2005 *Phys. Rev. A* **72** 012326
[25] Lo H K, Ma X F and Chen K 2005 *Phys. Rev. Lett.* **94** 230504
[26] Wang X B 2005 *Phys. Rev. Lett.* **94** 230503
[27] Wang X B 2005 *Phys. Rev. A* **72** 012322